Mon. Not. R. Astron. Soc. **278**, 209–218 (1996)

Local stability criterion for stars and gas in a galactic disc

Chanda J. Jog
Department of Physics, Indian Institute of Science, Bangalore 560012, India

Accepted 1995 August 2. Received 1995 July 17; in original form 1994 October 17

ABSTRACT

We obtain the criterion for local stability against axisymmetric perturbations in gravitationally coupled stars and gas in a galactic disc. The stars and gas are treated as two isothermal fluids, with the random velocity dispersion being higher in stars than in gas. The aim is to obtain a quantitative measure of the mutual destabilizing effect of the two components on each other. The problem is phrased in terms of a complete set of three dimensionless parameters: Q_s and Q_g, the standard Q parameters for local stability for stars alone and gas alone, respectively, and ε, the gas mass fraction in the disc. The results for Q_{s-g}, the two-fluid local stability parameter, and l_{s-g}, the dimensionless wavelength at which it is hardest to stabilize the two-fluid system, are obtained seminumerically as a function of Q_s, Q_g and ε and are presented as contour plots.

The Q_{s-g} values are lower than the one-fluid Q_s or Q_g values, especially for high gas fractions ($\varepsilon \geq 0.15$), indicating that the star–gas disc is more unstable than either constituent fluid by itself. l_{s-g} shows a bimodal distribution for low gas fractions ($\varepsilon \leq 0.1$) – that is, for low Q_s values l_{s-g} is in the stellar regime of high wavelengths, and vice versa. In contrast, for high gas fractions ($\varepsilon \geq 0.15$), the variation is smooth. Some applications of these results for the theoretical studies of stability and evolution of galaxies are discussed.

Key words: hydrodynamics – instabilities – galaxies: ISM – galaxies: kinematics and dynamics – galaxies: spiral.

1 INTRODUCTION

The standard criterion to denote stability against local, axisymmetric perturbations of a disc supported by differential rotation and random motion is

$$Q \equiv \frac{\kappa c}{\pi G \mu} > 1, \tag{1}$$

where κ is the local epicyclic frequency, c is the one-dimensional random velocity or the sound speed in the medium, and μ is the surface density. $Q=1$ indicates marginal or neutral stability, $Q<1$ indicates instability and $Q>1$ indicates stability as given above (Safronov 1960, Goldreich & Lynden-Bell 1965). A fluid representation of the component gives the above formula, while a distribution function or a kinetic theory approach gives a value of 3.36 instead of π in the above formula (Toomre 1964; Binney & Tremaine 1987). For a purely stellar or a purely gaseous disc, the appropriate values of c and μ are used, and the criterion for local stability in equation (1) is denoted by Q_s and Q_g respectively.

A real galactic disc, however, consists of two dynamically distinct components namely stars and gas, with the stars having a much larger velocity dispersion, c_s, than the gas, c_g. The two components are coupled gravitationally. Jog & Solomon (1984a,b; hereafter JS1, and JS2 respectively) studied the growth of local, axisymmetric perturbations in such a two-fluid (star–gas) galactic disc. They showed that owing to the low dispersion of gas ($c_g \ll c_s$), even only 10 per cent of the total disc density in the dynamically cold component (namely, gas) has a significant effect towards the destabilization of the entire star–gas disc. JS1 further showed that the range of wavelengths over which gravitational instabilities can occur is increased by the two-fluid interaction. Interestingly, these features would be seen in both stars and gas.

The importance of treating a galaxy as a two-component disc has also been pointed out by a number of other authors. The important effect of gas for the stability analysis of stars has been pointed out by Lynden-Bell (1967) and Smith & Miller (1986). The effect of stars in destabilizing a purely gaseous disc has been noted by Elmegreen (1987), Larson (1988), Kennicutt (1989) and Combes (1991); and in the case of active galactic nuclei, by Shlosman & Begelman (1988). Thus, it is not correct to use the standard one-component criterion for local stability as given by equation (1) while considering either stars or gas in a real galactic disc. It would be useful, therefore, to have a quantitative estimate of the mutual destabilizing effect of the two components on each other. This is the motivation for the present paper.

In this paper, we obtain the local stability criterion for a two-fluid (star plus gas) galactic disc, which is the two-fluid analogue of the result for a one-fluid disc given in equation (1). A related problem of local stability of a multicomponent system where each component is characterized by a different velocity dispersion, but for the case where there is no rotation in the system, was studied by Grishchuk & Zel'dovich (1981) and Fridman & Polyachenko (1984). A preliminary analysis of neutral or marginal equilibrium for a two-fluid disc supported by rotation and random motion was done by JS2 (see their fig. 1); also, see Nakamura (1978) and Bertin & Romeo (1988). These papers have only considered the limiting cases for Q_s above in which the two-fluid system is stable. However, a general analysis of the local stability of a two-fluid disc has not yet been done.

In this paper, we introduce physically meaningful dimensionless parameters and present a general analysis for the local stability of a star–gas disc for values covering the entire parameter space. Despite the symmetry in the problem, it does not yield a simple analytical criterion of local stability. Instead, we study the local stability problem seminumerically (Section 2). The contour plots for the resulting Q_{s-g}, the local stability parameter for a two-fluid star–gas disc, and l_{s-g}, the wavelength at which it is hardest to stabilize the two-fluid system, are presented in Section 3. Some possible applications of these results for theoretical studies of stability and evolution of galaxies are discussed in Section 4, and the conclusions from this paper are summarized in Section 5.

2 Q CRITERION FOR LOCAL STABILITY OF A STAR–GAS DISC

2.1 Neutral equilibrium

A normal-mode linear perturbation analysis of the two-fluid (star–gas) disc system supported by rotation and random motion (see JS1) showed that a radial mode (k, ω) obeys the following dispersion relation:

$$\omega^2(k)=\frac{1}{2}\{(\alpha_s+\alpha_g)-[(\alpha_s+\alpha_g)^2-4(\alpha_s\alpha_g-\beta_s\beta_g)]^{(1/2)}\}, \qquad (2)$$

where

$$\alpha_s=\kappa^2+k^2c_s^2-2\pi Gk\mu_s, \qquad \alpha_g=\kappa^2+k^2c_g^2-2\pi Gk\mu_g,$$
$$\beta_s=2\pi Gk\mu_s, \qquad \beta_g=2\pi Gk\mu_g. \qquad (3)$$

Here, k is the wavenumber $(=2\pi/\lambda$, where λ is the wavelength) and ω is the angular frequency of the perturbation.

In order that a two-fluid system be in a neutral equilibrium, $\omega^2(k)$ (as given by equation 2) $=0$, and the following equation must have a simultaneous real solution for k (see JS2):

$$\frac{\mathrm{d}[\omega^2(k)]}{\mathrm{d}k}=0. \qquad (4)$$

For a two-fluid system, the relation for ω^2 given by equation (2) is a fourth-order polynomial in k. Hence, in order to obtain the criterion for neutron equilibrium, we need to solve together a fourth-order polynomial, and a third-order polynomial (equation 4). As shown next, this is extremely tedious to perform analytically despite the obvious symmetry in the problem. An analytical solution for the neutral equilibrium would require that two roots of the biquadratic or the quartic in k be equal roots and the other two roots be imaginary such that $\omega^2 \geq 0$. This requires that $\Delta=I^3-27J^2=0$, and $I\neq 0$, $J\neq 0$ (Burnside & Panton 1960, p. 144) implying that $I>0$, $J\neq 0$ and $2HI-3aJ\geq 0$ (Burnside & Panton 1960, p. 153, example 31) – where the quantities H, I and J are expressions written in terms of the coefficients of the biquadratic and a is the coefficient of the fourth-order term in k. These expressions are complicated, and not amenable to a simple analytical solution. Hence, a simple analytical criterion for neutral equilibrium for a general two-fluid case is not feasible.

For the special limited range of parameters of very low $\varepsilon \ll 1$ and $Q_g \gg Q_s$, an analytical expression for the neutral equilibrium case has been obtained by Jog (1982) and Noguchi & Shlosman (1993). In this case, the two-fluid system may be treated as a small perturbation on the stars-alone case.

2.2 Q criterion – Q_{s-g}

For a one-fluid case, the value of $(k_{min})_{1-f}$ at which it is hardest to stabilize a system (corresponding to a minimum in ω^2) can be obtained trivially by solving $\mathrm{d}\omega^2/\mathrm{d}k=0$. This gives $(k_{min})_{1-f}=\pi G\mu/c^2$. Substituting this in the one-fluid dispersion relation it reduces to $\omega^2=(\kappa^2/Q^2)(Q^2-1)$. This gives $Q>1$ as the condition for local stability, as in equation (1), while $Q<1$ denotes local instability. A straightforward analytical extension of this procedure is not feasible for the two-fluid case, as discussed next.

For the two-fluid case, Elmegreen (1992) has formally rewritten ω^2 (from JS1) in terms of an effective Q factor and a multiplying function, both of which are written as functions of k'. Here, k' is a solution of $\mathrm{d}\omega^2/\mathrm{d}k=0$ that gives a minimum in ω^2. Elmegreen has shown that this Q parameter does reduce to the appropriate one-fluid value in the limits of $c_s=c_g$ and $\mu_g\to 0$. However, Elmegreen has not given an analytical expression for k' and hence for Q for the general case, except in a formal sense. Note that k' is a solution of a third-order polynomial, and hence could have one or three real solutions, and it is not easy to check analytically which of these correspond to a minimum in ω^2 (see the discussion in Section 2.1). In fact, the three solutions would need to be plugged into the expression for ω^2 (given by equation 2) to check this. The resulting general analytical Q criterion, which is not given by Elmegreen, would be cumbersome.

Instead, we treat this problem seminumerically. We obtain the solution for k_{min} corresponding to the minimum in ω^2 for the two-fluid case numerically. Next, we define the Q criterion for the general two-fluid case in terms of this, by making use of a relation obtained in JS1. This simplifies the treatment, and when combined with a physically meaningful set of dimensionless parameters, as in Section 3, it allows us to cover the full parameter space in a comprehensive fashion.

The approach we use is first illustrated for the case of a one-fluid disc. For the one-fluid disc, a function $F_{1\text{-f}}=2\pi Gk\mu/(\kappa^2+k^2c^2)$ is defined. From the one-fluid dispersion relation, it is clear that the system is stable, marginally stable or unstable at the given k depending on whether this function is <1, $=1$ or >1, respectively. Further note that at $(k_{\min})_{1\text{-f}}=\pi G\mu/c^2$, the above function $F_{1\text{-f}}$ is equal to $2/(1+Q^2)$. This result will be used later in this section to define the two-fluid Q parameter.

Recall from JS1 (their equations 21 and 22) that for a two-fluid system, ω^2 (as in equation 2) $=0$ is identical to setting the following function $F=1$, where

$$F=\frac{2\pi Gk\mu_{\rm s}}{\kappa^2+k^2c_{\rm s}^2}+\frac{2\pi Gk\mu_{\rm g}}{\kappa^2+k^2c_{\rm g}^2}. \tag{5}$$

Further, as shown in JS1, the necessary and sufficient condition that the two-fluid system be stable or unstable to the growth of axisymmetric perturbations at a given wavenumber k, is that F (as defined in equation 5) be <1 or >1, respectively. Note that this function for the two-fluid case is a linear superposition of the terms for the stars-alone and gas-alone cases respectively.

Now, $k_{\min}$ is the wavenumber at which it is hardest to stabilize the two-fluid system, since it corresponds to a minimum in ω^2 (given by equation 2). Therefore, for a given set of input parameters, the two-fluid system is stable over all wavelengths, or is marginally stable, or is unstable over a range of wavelengths; depending on whether the function F (in equation 5) obtained at $k_{\min}$ is <1, $=1$ or >1 respectively. Define $Q_{\rm s\text{-}g}$ to be the indicator of local stability against axisymmetric perturbations in a two-fluid star–gas disc system supported by rotation and random motion. In a direct analogy with the one-fluid case discussed above, we define $Q_{\rm s\text{-}g}$ to be

$$[F]_{\text{at } k_{\min}}\equiv\frac{2}{1+(Q_{\rm s\text{-}g})^2}. \tag{6}$$

The necessary and sufficient condition for the two-fluid system to be stable, marginally stable, or unstable is given by $Q_{\rm s\text{-}g}>1$, $=1$ or <1 respectively.

This direct extension for the two-fluid case is possible because the function F (equation 5) for the two-fluid case is a linear superposition of the terms for the stars-alone and gas-alone cases respectively. Thus $Q_{\rm s\text{-}g}$ is determined by the contributions of stars and gas at $k_{\min}$.

We check that in the limit of $\mu_{\rm g}\to 0$, the second term on the right-hand side of equation (5) drops out and $k_{\min}$ is given by the stars-alone value to be $=\pi G\mu_{\rm s}/c_{\rm s}^2$, where $\mu_{\rm s}$ in this case is the total disc surface density. In this limit, $Q_{\rm s\text{-}g}$ as defined by equation (6) does indeed reduce to $Q_{\rm s}$, as expected. Also, we check that in the limit of $c_{\rm s}=c_{\rm g}$, the denominators of the two terms on the right-hand side of equation (5) are identical and these two terms add to yield an expression for Q for a one-component system, as expected.

In fact, the above approach may be extended in a straightforward way to an n-component disc system by writing F (equation 5) as a linear superposition of the corresponding one-fluid terms, and obtaining $k_{\min}$ numerically for the appropriate dispersion relation. Thus we may obtain $Q_{1,2,\ldots,n}$ for n gravitationally coupled components in a disc supported by rotation and random motion. This will be pursued in a future paper.

For the special case of two weakly interacting fluids, an analytical expression for the two-fluid Q parameter has been derived by Wang & Silk (1994). However, their analytical Q criterion is invalid since they have used a wrong definition of $Q[=(F)^{-1}]$, and further they have incorrectly added the contributions of the two fluids at their respective neutral wavenumbers rather than calculating both of these terms at a *common* two-fluid $k_{\min}$. Their result for the two-fluid Q (see their equation A16) is therefore wrong – for example, their Q is independent of the gas fraction, ε, which is not physically meaningful.

We next introduce a complete set of three dimensionless parameters for this problem, namely $Q_{\rm s}$, $Q_{\rm g}$, the standard Q parameters for local stability for stars-alone and gas-alone respectively (see Section 1), and $\varepsilon=\mu_{\rm g}/(\mu_{\rm s}+\mu_{\rm g})$, the gas mass fraction in the galactic disc. $l=[\kappa^2/2\pi Gk(\mu_{\rm s}+\mu_{\rm g})]$ is the dimensionless measure of the wavelength of the perturbation. Writing equation (6) in terms of these, $Q_{\rm s\text{-}g}$, the local stability parameter for the two-fluid case is defined to be

$$\frac{(1-\varepsilon)}{l_{\rm s\text{-}g}\{1+[Q_{\rm s}^2(1-\varepsilon)^2]/(l_{\rm s\text{-}g}^2 4)\}}+\frac{\varepsilon}{l_{\rm s\text{-}g}[1+Q_{\rm g}^2\varepsilon^2/(l_{\rm s\text{-}g}^2 4)]}\equiv\frac{2}{1+(Q_{\rm s\text{-}g})^2} \tag{7}$$

where $l_{\rm s\text{-}g}=[\kappa^2/2\pi Gk_{\min}(\mu_{\rm s}+\mu_{\rm g})]$ is the dimensionless wavelength at which it is hardest to stabilize the two-fluid system. The dimensionless 'minimum' wavelengths at which it is hardest to stabilize the gas-alone and the stars-alone cases are given respectively by $l_{\rm g}=(2c_{\rm g}^2/G\mu_{\rm g})[\kappa^2/4\pi^2G(\mu_{\rm s}+\mu_{\rm g})]=Q_{\rm g}^2\varepsilon/2$ and $l_{\rm s}=Q_{\rm s}^2(1-\varepsilon)/2$ respectively. Recall from JS1 that $l_{\rm s\text{-}g}$ lies between $l_{\rm g}$ and $l_{\rm s}$ because the joint two-fluid system is more unstable than either fluid by itself. These limits are used to obtain $Q_{\rm s\text{-}g}$ following the procedure as described next.

For a given set of values of the input parameters $Q_{\rm s}$, $Q_{\rm g}$ and ε, we obtain numerically the minimum value of the dimensionless dispersion relation (ω^2/κ^2) for the two-fluid case, for the l values covering the range from $l_{\rm g}$ to $l_{\rm s}$. This gives the value of $l_{\rm s\text{-}g}$. Plugging this into equation (7) yields the value of $Q_{\rm s\text{-}g}$. Thus, we get both $Q_{\rm s\text{-}g}$ and $l_{\rm s\text{-}g}$ for a given set of values for the input parameters. The resulting $Q_{\rm s\text{-}g}$ and $l_{\rm s\text{-}g}$ are presented as contour plots in Section 3.

3 RESULTS

3.1 $Q_{\rm s\text{-}g}$ for a star–gas system

Following the procedure as in Section 2.2, we obtain $Q_{\rm s\text{-}g}$ as a function of $Q_{\rm s}$, $Q_{\rm g}$, each of which covers a range from 1 to 2.5. The upper limit of 2.5 used follows from the fact that a real galactic disc is believed to be self-regulated and hence the Q values are expected to be ≤ 2–3 (Goldreich & Lynden-

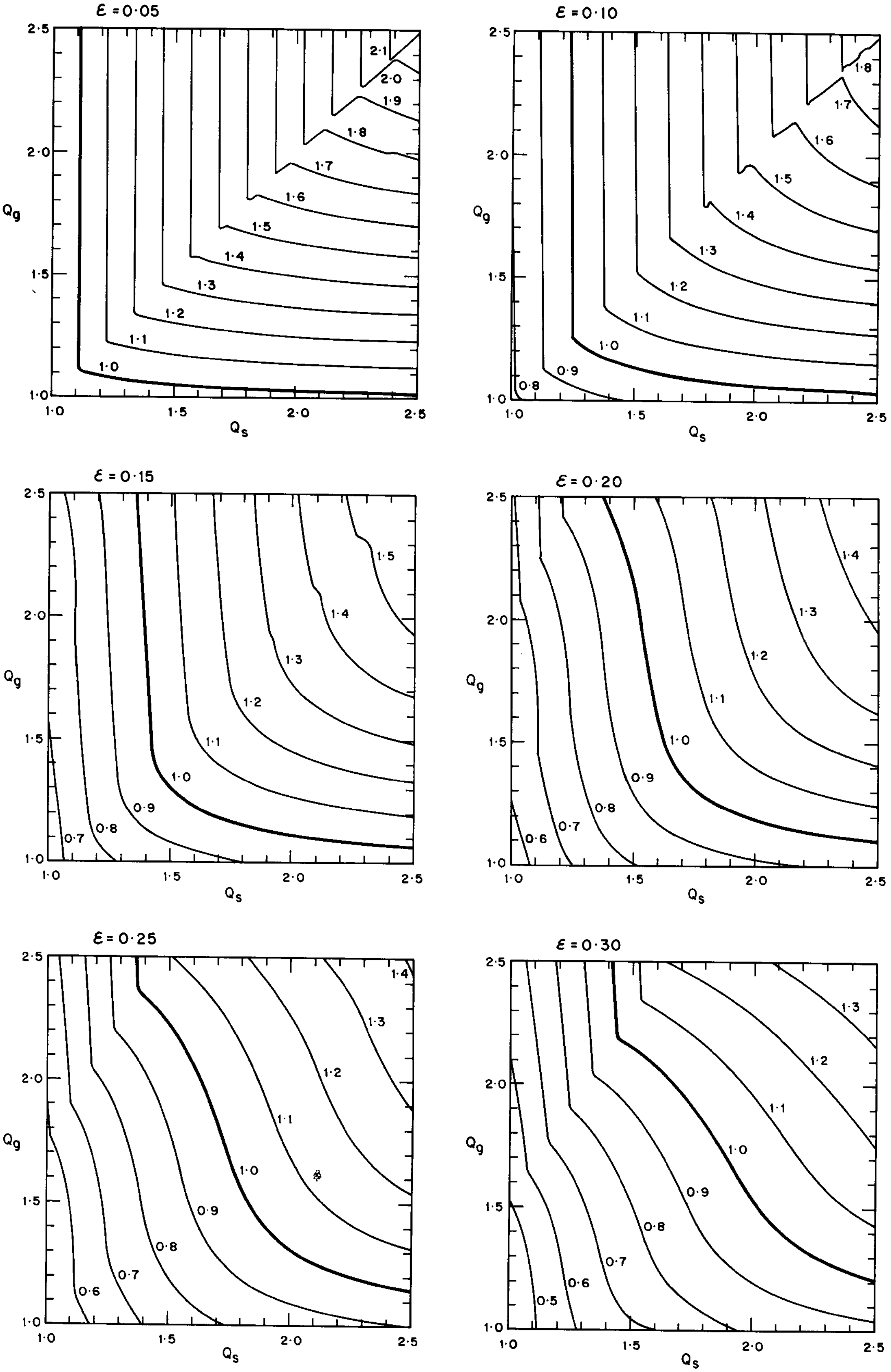

Figure 1. A contour plot of $Q_{s\text{-}g}$, the local stability parameter for a two-fluid star–gas disc, given as a function of Q_s and Q_g. The gas mass fraction, ε, is set equal to 0.05, 0.10, 0.15, 0.20, 0.25 and 0.30 in Figs 1(a)–(f) respectively.

$Q_{s\text{-}g}$ is smaller than the corresponding one-fluid Q_s or Q_g values – especially at the higher gas fractions, $\varepsilon \geq 0.15$. The bold contour denotes two-fluid neutral equilibrium in each case, and it separates the stable regime to the right of it from the unstable regime to the left of it.

Bell 1965; Sellwood & Carlberg 1984). Fig. 1 contains contour plots for Q_{s-g} given as functions of Q_s and Q_g for the gas fraction, $\varepsilon = 0.05$, 0.1, 0.15, 0.2, 0.25 and 0.3 (Figs 1a–f respectively). The ε values 0.05–0.25 cover the observed range of values for the gas fractions (e.g., Young 1990). The case $\varepsilon = 0.3$ is plotted as an example of an extreme gas-rich galaxy to illustrate that such galaxies cannot be stable (see Section 4.2).

3.1.1 Q_{s-g} *versus one-fluid Q values*

The resulting Q_{s-g} values are always lower than the corresponding one-fluid Q_s or Q_g values, especially at high gas fractions ($\varepsilon \geq 0.15$), indicating that the two-fluid system is more unstable than either constituent fluid in the system by itself. This is a result of the gravitational interaction between stars and gas. Owing to the low gas dispersion, even a gas fraction $\varepsilon \sim 0.1$–$0.15 \ll 1$ significantly destabilizes the entire star–gas two-fluid disc. Thus it is not correct to use the standard one-component (Toomre) criterion for local stability as given by equation (1) to denote the stability of stars and gas in a real coupled star–gas galactic disc. Instead, in general, the two-fluid stability parameter values as given by the contour plots for Q_{s-g} must be used. Implications of these results for the stability and evolution of galaxies are given in Section 4.

If one were to consider a purely stellar disc of the same total surface density, so that $\varepsilon = 0$ and $\mu_s = \mu_t$, then $Q_{s-g} = Q_s$ as shown in Section 2.2. In this limit, $Q_g \gg Q_s$. Conversely, in the other limit of a purely gaseous disc ($\varepsilon = 1$), it follows from equation (5) that $Q_{s-g} = Q_g$ where $\mu_g = \mu_t$. In this limit, $Q_s \gg Q_g$. Note that Q_{s-g} for a real two-fluid disc (as given by equation 6) lies between the above two limits. That is, the two-fluid system is more unstable than a purely stellar disc and is less unstable than a purely gaseous disc of the same total surface density.

However, when studying the stability of a real two-fluid star–gas disc of non-zero stellar and gas densities, it is more meaningful to compare the resulting Q_{s-g} with the finite, single-fluid Q values that characterize the constituent fluids: namely Q_s and Q_g, as we have done in this Section. We find that Q_{s-g} is always less than Q_s and Q_g, indicating that the joint two-fluid system is more unstable than either constituent fluid by itself, with parameters as in the real two-fluid disc.

3.1.2 *Two-fluid neutral equilibrium*

The bold contour for each case in Fig. 1 represents $Q_{s-g} = 1$, which denotes two-fluid neutral or marginal equilibrium. The region to the right of this contour in the Q_s–Q_g plane denotes the Q values for which the two-fluid system is stable, whereas the region on the left denotes an unstable system. At a given value of Q_g, the range of Q_s values over which the two-fluid system is unstable – that is, the region to the left of the bold contour – increases as ε is increased. This is a result of the increasing importance of gas contribution. This is especially evident at low Q_g values.

The use of dimensionless parameters and their optical choice (Section 2.2) allows us to explore easily the full parameter range in a comprehensive fashion. In contrast, the preliminary study of local neutral equilibrium in JS2 was restricted to a few cases where κ, μ_t and c_g was kept constant and ε was varied to study the effects of variation of Q_g. Thus the only regimes explored earlier in JS2 or in the work by others were characterized by either low ε, high Q_g and low Q_s (see e.g. JS2, or Noguchi & Shlosman 1993), or high ε, low Q_g and low Q_s.

3.2 l_{s-g} for a star–gas system

In this section, we present contour plots for l_{s-g}, given as functions of Q_s and Q_g each varying between 1 to 2.5, for a gas fraction $\varepsilon = 0.05$, 0.1, 0.15 and 0.2 (Figs 2a–d respectively). The values for l_{s-g} were obtained following the numerical procedure as outlined in Section 2.2.

The bold contour in Fig. 2 is the contour corresponding to $Q_{s-g} = 1$ from Fig. 1. The l_{s-g} values on the left-hand side of the contour for $Q_{s-g} = 1$ give the most unstable wavelengths, that is, they correspond to the fastest growing two-fluid modes. These modes would occur in both stars and gas. These may be compared with the observed values of linear features in stars and gas in galaxies (see Section 4.3 for details). The modes on the right-hand side of this bold contour are stable. The l_{s-g} values corresponding to the contour $Q_{s-g} = 1$ give the two-fluid neutral wavelengths.

3.2.1 l_{s-g} *versus one-fluid l values*

Fig. 2 shows that at low Q_g values, the l_{s-g} values for the two-fluid system are small, close to l_g, the one-fluid, gas-alone values. Conversely, for high Q_g values, the l_{s-g} values are high, close to l_s, the one-fluid, stars-alone values. This shift is a generalization of the result shown for a specific set of parameters in fig. 4 of JS1. This shift can be understood in terms of the relative contributions of gas and stars at l_{s-g} (the ratio of the second and the first term on the right-hand side of equation 7). This ratio is high, that is, the gas contribution dominates over the stellar contribution at l_{s-g}, for high Q_s and low Q_g values. For this parameter range, the value of l_{s-g} is mainly determined by the gas contribution. Conversely, for high Q_g and low Q_s values, the stellar contribution dominates and hence it determines the value for l_{s-g} (see Fig. 2).

3.2.2 *Variation in* l_{s-g} *with* ε

An interesting result is that at low gas fractions ($\varepsilon = 0.05$, 0.1) – see Figs 2(a) and (b) – the transition from low to high values in l_{s-g} is sharp. That is, it occurs over a small range of Q_s and Q_g values. In contrast, this transition is gradual at high $\varepsilon (= 0.15$, 0.2) – see Figs 2(c) and (d). This difference is especially striking given that a larger contour interval of 0.8 is used for clarity in Fig. 2(a), while that in Fig. 2(b) is 0.4; and that in Figs 2(c) and (d) is even smaller, i.e., 0.10.

At low $\varepsilon (\leq 0.1)$, the two-fluid system is clearly either in a gas-dominated regime or in a star-dominated regime over most of the Q_s, Q_g range. Only in the sharp transition zone are the contributions from the two fluids comparable, to within a factor of a few of each other. This explains why l_{s-g} and Q_{s-g} are nearly independent of Q_s below a certain Q_g, and vice versa for the low gas fractions.

Conversely, the transition in l_{s-g} from l_g to l_s is smooth at higher gas fractions ($\varepsilon \geq 0.15$) – see, for example, Figs 2(c) or (d). This happens for the following reasons. First, the

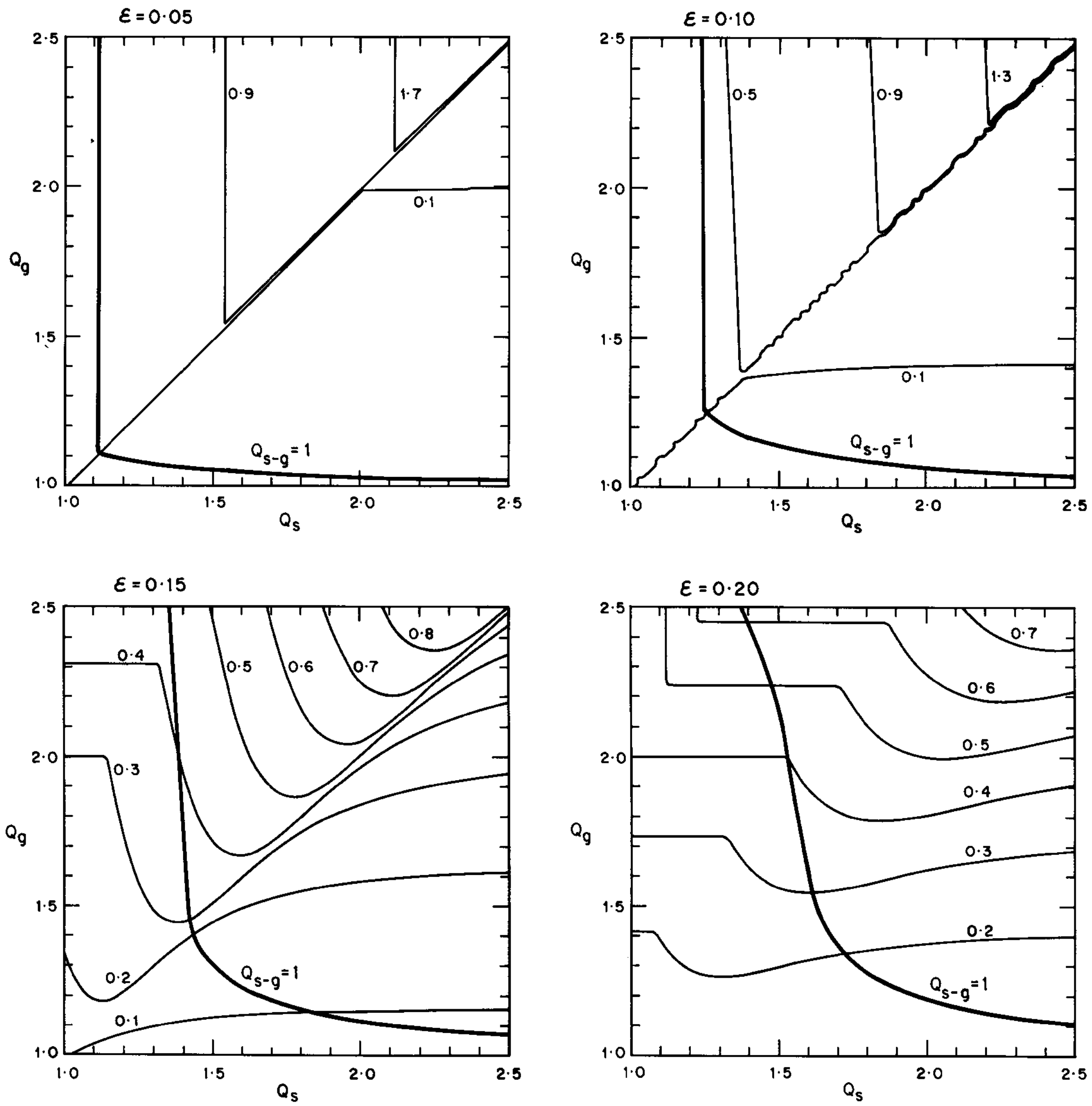

Figure 2. A contour plot of $l_{s\text{-}g}$, the dimensionless wavelength at which it is hardest to stabilize the two-fluid star–gas disc, given as a function of Q_s and Q_g, for the gas fraction $\varepsilon = 0.05$, 0.10, 0.15 and 0.2 – in Figs 2(a)–(d) respectively. The bold curve represents $Q_{s\text{-}g} = 1$, denoting neutral equilibrium, and is superimposed from Fig. 1. The $l_{s\text{-}g}$ values to the left of it denote the most unstable wavelengths.

The variation in $l_{s\text{-}g}$ from low to high values is sharp at low gas fractions (Figs 2a–b), whereas the variation is smooth at high gas fractions (Figs 2c–d). This is especially striking given the higher contour intervals used for clarity in Figs 2(a) and (b).

'minimum' l values for the individual components ($l_g = Q_g^2 \varepsilon/2$ and $l_s = Q_s^2(1-\varepsilon)/2$ – see Section 2.2) are closer at high ε. This leads to an increase in the contribution by each fluid at the 'λ domain' of the other fluid. Also, the resulting range of contour levels for $l_{s\text{-}g}$ for the two-fluid case is smaller (see Fig. 2). Secondly, at high ε, the gas contribution towards formation of instabilities is important and it dominates over a larger range of wavelengths. This last point was shown for a particular set of input parameters by JS1 (see their fig. 4). Hence, at high $\varepsilon (\geq 0.15)$, the contours for $l_{s\text{-}g}$ vary gradually with Q_s and Q_g. Thus the behaviour of $l_{s\text{-}g}$ is qualitatively different for $\varepsilon \geq 0.15$. Owing to the lower gas dispersion ($c_g \ll c_s$, that is, $Q_g \varepsilon \ll Q_s(1-\varepsilon)$ – see Section 2), this different behaviour is seen when the gas fraction is only $\geq 0.15 (\ll 1)$. Observational implications of this result are discussed in Section 4.3.

3.2.3 $l_{s\text{-}g}$ *in the gas regime at low* ε

A surprising result is that even for small ε, equal to, say, 0.05, the value of $l_{s\text{-}g}$ could be small $\sim l_g$, that is in the gas-dominated regime, when the Q_s values are high and the Q_g values are low (≥ 1) (Fig. 2a). This is contrary to the naïve expectation that for low gas fractions, $l_{s\text{-}g}$ would be in the stellar regime. Hence a simple analytical parametrization of the two-fluid Q criterion (assuming $l_{s\text{-}g}$ to be $\sim l_s$) is not possible, in general, even for low gas fractions ($\varepsilon \leq 0.1$). This regime of low ε, high Q_s and low Q_g was not explored earlier by JS1 or others (see Section 3.1.2). See Section 4.3 for observational implications of this result.

3.3 Shapes of contours

At a given ε, as Q_s decreases, Q_g has to increase to maintain a constant value of $Q_{s\text{-}g}$. This is as expected, since the two fluids together contribute to the unstable behaviour of the two-fluid system (Section 2.2). At low $\varepsilon \le 0.1$, and low Q_g, the resulting $Q_{s\text{-}g}$ is nearly independent of Q_s and vice versa. At low gas fractions, the gas contribution is not important for low Q_s values, since in this case $l_{s\text{-}g} \sim l_s$. Hence the contours are sharper for low Q_s values than for low Q_g values. Conversely, at high gas fractions, the gas contribution is important and even dominates, and hence the contours at low Q_s are less sharp than at low Q_g values.

The double-humped behaviour of the $Q_{s\text{-}g}$ contours at low ε, and high Q_s and high Q_g values can be explained based on the variation in the $l_{s\text{-}g}$ values as given next. For this regime, the l_g and l_s values at which it is hardest to stabilize gas-alone and stars-alone systems (see Section 2.2. for their definitions), are far apart. Hence each fluid contributes little in the wavelength range of the other fluid. Thus, a large range of values in $l_{s\text{-}g}$ is spanned in the crossover zone from the star-dominated to the gas-dominated regime (see Fig. 2a and b). Hence the values of $Q_{s\text{-}g}$ in this regime, as determined by both the terms on the right-hand side of equation (7), result in the double-humped behaviour for the $Q_{s\text{-}g}$ contours. For the lowest $\varepsilon = 0.05$, and higher Q_s values, this behaviour is seen even more clearly, since l_g and l_s are even further apart in this regime. Conversely, at low $\varepsilon(=0.05$ and $0.1)$, and low Q_s and low Q_g values, the range in $l_{s\text{-}g}$ in the crossover zone is small. In this case the two terms on the right-hand side of equation (7) combine to give the smooth contours for $Q_{s\text{-}g}$, as observed in Fig. 1. Also, at higher $\varepsilon(\ge 0.15)$, and for all Q_s and Q_g values, the transition from the gaseous to the stellar regime – that is, $l_{s\text{-}g}$ going from $l_g \rightarrow l_s$ – is smooth (see Section 3.2.2). Hence the resulting contours for $Q_{s\text{-}g}$ are smooth and do not show any evidence for the double-humped behaviour. Note that, in any case, the function $Q_{s\text{-}g}$ is single-valued for a given set of values for Q_s, Q_g and ε. Also, the double-humped behaviour does not have direct observational implications, since it occurs when $Q_{s\text{-}g} > 1$.

The detailed variation of $l_{s\text{-}g}$ contours can be understood in terms of the relative contributions from the two fluids. For example, at $\varepsilon = 0.05$, and low Q_g values, say ≥ 1, and high Q_s values, say ~ 2–2.5, the gas contribution is dominant and hence a contour for $l_{s\text{-}g}$ is flat (independent of Q_s). Below a certain Q_s, however, the stellar contribution starts to become important and hence lower values of Q_g are required to maintain the contour at a given $l_{s\text{-}g}$. The behaviour in the stellar-dominated region of higher wavelengths can be explained in a similar fashion.

At low gas fractions, the contours for $l_{s\text{-}g}$ are closer at high Q_s and Q_g values. This is because in this case, the l_g–l_s range is high, and hence the range of $l_{s\text{-}g}$ values covered is high. Conversely, at high fractions, the range in l_g–l_s, and hence the resulting range in $l_{s\text{-}g}$, is small (see Section 3.2.2). Therefore, in this case, the contours for $l_{s\text{-}g}$, and hence for $Q_{s\text{-}g}$, vary gradually with Q_s and Q_g.

3.4 Discussion

In the above analysis, we have assumed an infinitesimally thin disc for mathematical convenience. The net result of a finite scaleheight $(2h)$ would be to reduce the effective surface density of that particular component, with a reduction factor of $[1-\exp(kh)]/kh$ (Toomre 1964; JS1) which is more important for stars than for gas. Thus, neglecting the finite stellar scaleheight as done here slightly underestimates the Q_s and hence the $Q_{s\text{-}g}$ values, especially in the gaseous regime of small $l_{s\text{-}g} \sim l_g$ values (corresponding to low Q_g and high Q_s values).

In the present work, the velocity dispersion in gas is assumed to be smaller than that in stars (see Section 2.2). We ensure that the range of values chosen for Q_s, Q_g and ε do in fact satisfy the relation

$$\frac{c_g}{c_s} = \frac{Q_g \varepsilon}{Q_s(1-\varepsilon)} < 1. \tag{8}$$

This is valid except for the lowest Q_s and the highest Q_g values for the very high ε values treated in Figs 1(e) and (f).

4 APPLICATIONS

In Section 3, we have presented quantitative results for $Q_{s\text{-}g}$ and $l_{s\text{-}g}$ in terms of the three dimensionless input parameters (Q_s, Q_g, ε), for the entire parameter space. In this section, we discuss some possible applications of these results.

4.1 $Q_{s\text{-}g}$ values for galaxies

4.1.1 $Q_{s\text{-}g}$ versus radius for the Galaxy

A direct application is to use them to obtain the radial profile of $Q_{s\text{-}g}$ for the Milky Way and for external galaxies for which observational data for the input parameters are available. The measurement of the stellar velocity dispersion is particularly difficult (e.g., Lewis & Freeman 1989, Bottema 1989). Such a stability profile would tell one at a glance which region of a galaxy is most unstable to the growth of axisymmetric gravitational perturbations. These results for $Q_{s\text{-}g}$ would be of interest for dynamical studies of galaxies. For example, in the past it has been claimed that a one-fluid stellar galaxy would evolve until it is barely stable to local axisymmetric perturbations, that is, $Q_s \ge 1$ (e.g., Binney & Tremaine 1987). A real two-fluid (star–gas) galactic disc would probably evolve until $Q_{s\text{-}g} \ge 1$, as was first proposed by Goldreich & Lynden-Bell (1965). Next, we check if this is true for the Galaxy by calculating $Q_{s\text{-}g}$ at various radii.

For the Galaxy, Q_s values have been obtained by Lewis & Freeman (1989) from observations of stellar velocities in low-absorption (Baade) windows. The values for the observed total neutral gas densities are taken from Scoville & Sanders (1987). The values for κ and μ_t are taken from the mass model for the Galaxy by Caldwell & Ostriker (1981). From these, we obtain the values of the gas fraction, ε, and Q_g as a function of radius. These, and the resulting values of $Q_{s\text{-}g}$ versus the radius, R, in the galactic disc are presented in Table 1. The Sun is taken to be at $R = 8.5$ kpc.

The resulting values of $Q_{s\text{-}g}$ are lower than the corresponding Q_s and Q_g values. Note that $Q_{s\text{-}g} \ge 1.1$ for $R = 4$ to

Table 1. Q_{s-g} versus radius for the Galaxy.

R (kpc)	ϵ	Q_s	Q_g	Q_{s-g}
4	0.07	1.9	1.5	1.4
5	0.09	1.9	1.2	1.1
6	0.09	1.8	1.4	1.2
7	0.08	1.6	1.6	1.3
8	0.10	1.6	1.5	1.2
8.5	0.09	1.5	1.8	1.2

8.5 kpc. Thus, the two-fluid galactic disc is close to neutral equilibrium over most of the inner Galaxy. This confirms the prediction for a self-regulated galaxy proposed by Goldreich & Lynden-Bell (1965). The Galaxy is closest to being unstable to the growth of two-fluid axisymmetric perturbations in the range $R=4$ to 6 kpc. This is the region where the gas density values are the highest in the Galaxy. Note that this coincides with the molecular ring region in the Galaxy (e.g., Scoville & Sanders 1987). Thus, even when the gas by itself is stable, if Q_{s-g} were less than 1 then the joint two-fluid system would help in the growth of gas instabilities in the ring region via induced gas instabilities as in JS2.

The actual values of Q_{s-g}, and hence the radial range over which Q_{s-g} is close to or less than 1, have substantial error bars because of the errors in the input parameters, and also because different mass models were used to obtain the values of Q_s and Q_g.

4.1.2 *Stability of star–gas galactic discs*

In studies of galactic dynamics, Q_s is generally used as a handy quantitative indicator of dynamical stability of the disc (e.g., Binney & Tremaine 1987). The recent trend in the literature is to tackle the formation and evolution of more realistic galaxies, which take into account the gas dynamical effects (e.g., Evrard 1993, also Section 1). In Section 3.1.1, we have shown that the two-fluid Q_{s-g} values are always lower than the corresponding Q_s and Q_g values for the constituent single fluids. Future theoretical studies of the stability and evolution of discs of galaxies should therefore incorporate Q_{s-g}, as given by Fig. 1 (rather than Q_s or Q_g), as the quantitative measure of the joint two-fluid disc stability. This would be particularly important for the studies of the early evolution of galaxies when the discs would be much more gas-rich.

For studying the growth via swing amplification of non-axisymmetric two-fluid perturbations, one needs to consider a system which is stable to axisymmetric perturbations, that is, with $Q_{s-g}>1$ (Jog 1992). The results for Q_{s-g} in Fig. 1 provide a ready list of initial parameters for such studies.

4.2 Stability as a function of gas fraction ε

4.2.1 *Stability of gas-rich galaxies*

From Fig. 1(f) corresponding to the gas fraction $\varepsilon=0.3$, it can be seen that the two-fluid system is unstable ($Q_{s-g}\leq 1$), for a large fraction of the range of observed values for Q_s and Q_g (each ≤ 2.5 – see Section 3.1). Such a galaxy would evolve rapidly until a lower gas fraction is achieved. Therefore, we expect that gas-rich, large spiral galaxies with $\varepsilon \geq 0.3$ will not be seen at the present epoch. This expectation is confirmed by the observational data on the gas content of galaxies. It is well known that the gas fraction is higher for the late-type galaxies than for the early-type galaxies. Even for the most gas-rich, late-type spiral galaxies such as Scd–Im, the mean value of ε is 0.25 (Young 1990; Roberts & Haynes 1994).

In fact, even for a slightly smaller gas fraction ($\varepsilon=0.25$, see Fig. 1e), the two-fluid system is stable over only a small range of values for Q_s and Q_g (e.g., for $Q_s \geq 2.2$ when $Q_g \leq 1.2$). For a gas-rich galaxy, such high values of Q_s are possible only if μ_t, the total surface density, is low. Therefore, we predict that a gas-rich galaxy (with $\varepsilon \geq 0.25$) would only be stable if it had a low total surface density. This is confirmed by observations since the typical, gas-rich late type galaxies of type Scd–Im are small in size and are observed to have low surface densities compared with the early-type galaxies (e.g., Roberts & Haynes 1994).

An extreme and rare example of this behaviour is seen in the gas-rich, giant but low surface brightness galaxies such as Malin 1. Malin 1 has a high gas mass fraction of over 0.5 but it has a very low gas surface density of $\sim 2\ M_\odot\ pc^{-2}$ (Impey & Bothun 1989). Hence such a galaxy would be stable against gas-alone and even star–gas instabilities. This explains why such gas-rich giant galaxies are stable and have a low surface brightness indicating an overall low star formation over its lifetime. In any case, galaxies such as Malin 1 appear to be rare at the present epoch.

4.2.2 *Gas depletion*

As an additional use of these figures, one could study the evolution in these plots (Figs 1 and 2) of a galaxy in which the gas is being consumed and the gas fraction is decreasing with time (also see Section 4.3.1). This may be applied, for example, to an evolving galactic disc (e.g., Chamcham, Pitts & Taylor 1993), or to an evolving star–gas disc in an active galactic nucleus (e.g., Shlosman & Begelman 1989).

4.3 Sizes of star–gas features in galaxies

Recall from Section 3.2 that the l_{s-g} values to the left of the bold contour in Fig. 2 correspond to the most unstable two-fluid wavelengths. These features will be seen in both stars and gas. Fig. 2 shows that l_{s-g} varies smoothly with Q_s and Q_g at high ε (≥ 0.15), whereas the transition is sharp at low gas fractions. This variation with ε has interesting observational implications, as discussed next.

4.3.1 *Large range in sizes of features at high ε*

First, a given region of a gas-poor galaxy would be in either a gas-dominated regime of low l_{s-g} or in a star-dominated regime of high $l_{s\text{-}g}$. In contrast, gas-rich galaxies would be expected to display two-fluid features in stars and gas over a large range of wavelengths. This is despite the fact that the range of $l_{s\text{-}g}$ is lower for higher gas fraction (for the same range in Q_s and Q_g) – see Section 3.2.2. This can explain the observed patchy, fragmented appearance – with fragments of different sizes – of the late-type and irregular galaxies as seen for example in M101 (NGC 5457) or in M33 (NGC 598) (e.g., Sandage 1961). Further, one expects to see a larger range of wavelengths for features at the early stages in the evolution of all galaxies. The smooth variation with Q in $l_{s\text{-}g}$ at high gas fractions (Fig. 2) points to a smooth early dynamical evolution of galaxies.

4.3.2 *Features in gas-domain at low ε*

A completely new regime explored in the current work is that of low ε and low Q_g, for which the $l_{s\text{-}g}$ is small $\sim l_g$, that is, it is in the gas-dominated regime. Given the fairly robust behaviour of the cloud velocity dispersion (Jog & Ostriker 1988), this set of values are likely to be applicable to gas-poor, high total surface density regions as in the inner regions of early-type galaxies. Thus we can explain the many small segments seen in the morphology of an Sa or Sb such as NGC 3898 or NGC 2841 (e.g., Sandage 1961) as material features in stars and gas.

4.3.3 *Feature size in the Galaxy*

At $R = 5$ kpc in the Galaxy, $Q_{s\text{-}g} = 1.1$ (see Table 1, Section 4.1.1), so that the Galaxy is barely stable to axisymmetric perturbations. If the Galaxy were to be barely unstable (and this is possible given the large error bars in $Q_{s\text{-}g}$ as discussed in Section 4.1.1), then $l_{s\text{-}g} \leq 0.1$ (see Fig. 2b). From the definition of the dimensionless wavelength (Section 2.2), and on using the values for κ and μ_t at $R = 5$ kpc obtained (from Caldwell & Ostriker 1981) earlier in Section 4.1.1, we get the corresponding wavelength for the star–gas features to be ≤ 0.9 kpc. This is much smaller than the size of a one-fluid stellar instability in the Galaxy, which is ~ 5–8 kpc (Toomre 1964). Note that the resulting two-fluid scale, $\sim$kpc, is in better agreement with the typical small-scale features seen in spiral galaxies.

Recall that $l_{s\text{-}g}$ represents the size of perturbation in both stars and gas. Recent advances in the near-infrared and mm-wave interferometry would now allow high-resolution ($\sim$a few arcsec) mapping of stellar and gas features respectively for a large number of galaxies (e.g., Sargent & Welch 1993). At these resolutions, it is possible to map features of $\sim$kpc size as far away as the Virgo cluster centre. Such simultaneous mapping in future can give accurate measurements of $l_{s\text{-}g}$ which can be compared with the results from the present paper (e.g., as given in Sections 4.3.1 and 4.3.2).

4.3.4 *Star–gas features in galaxies with gas infall*

Another application of results in Section 3 would be to see how the two-fluid stability is affected in interacting galaxies. An interesting point is that if gas were to be added to a galaxy in an interaction or as a result of external gas infall, then $l_{s\text{-}g}$ may change abruptly from $\sim l_s$ to $\sim l_g$ for a gas-poor galaxy such as an Sa, whereas a large gas-rich galaxy such as an Sc would be only marginally affected in either its gas content or in the range of values for the instabilities displayed.

4.4 Critical gas density for star formation

Kennicutt (1989) has shown from a study of a number of galaxies that the star formation rate seems to show a cut-off below the critical gas density given by $\alpha Q_g > 1$, where $Q_g \geq 1$ is the one-fluid gas-alone local stability criterion, and $\alpha = 0.67$. The factor α is meant to represent the effect of the star–gas interaction in an average sense. Chamcham et al. (1993) have further explored this concept of threshold or critical gas density, and have performed a detailed modelling of the chemical evolution of galactic discs. In view of the destabilizing effect of the star–gas interaction on either fluid (Section 3), we believe that if a plot of the star formation rate versus critical μ_g (corresponding to $Q_{s\text{-}g} = 1$) were to be made, it would show a transition at lower gas surface densities. The difference from Kennicutt's results is expected to be most apparent when the stellar contribution is important, as would be the case for low Q_s and high Q_g values, and low gas fractions. Alternatively, it could also be that the critical gas density as given by the local disc stability is not a sufficient criterion for the onset of star formation within interstellar clouds. This may instead depend on other, non-linear, microscopic processes within the clouds such as turbulence (e.g, Bonazzola et al. 1987).

5 SUMMARY

We obtain the local stability criterion for gravitationally coupled stars and gas in a galactic disc, with the stars having a higher velocity dispersion than the gas. The two-fluid system is stable, marginally stable, or is unstable depending on whether $Q_{s\text{-}g}$, the two-fluid local stability parameter, is > 1, $= 1$ or < 1 respectively. The resulting contour plots for $Q_{s\text{-}g}$, and $l_{s\text{-}g}$, the wavelength at which it is hardest to stabilize the two-fluid system, are given as functions of Q_s, Q_g – the standard Q parameters for local stability for stars-alone and gas-alone respectively, and ε, the gas mass fraction in the disc, for values covering the entire parameter space. $l_{s\text{-}g}$ represents the wavelength for perturbation in both stars and gas.

The resulting values of $Q_{s\text{-}g}$ are lower than the one-fluid Q_s or Q_g values, indicating that the two-fluid system is more unstable than either constituent fluid in the system by itself. Owing to its lower velocity dispersion, gas has a significant destabilizing effect on the entire star–gas disc even when the gas fraction is only ~ 0.1–0.15 ($\ll 1$). Therefore, while studying the stability of a real two-fluid galactic disc, the two-fluid $Q_{s\text{-}g}$ results given here should be used instead of the single-fluid Q_s or Q_g values. $l_{s\text{-}g}$ shows a bimodal distribution for low gas fractions ($\varepsilon \leq 0.1$) – namely, for low Q_s and high Q_g values, $l_{s\text{-}g}$ is in the stellar regime of high wavelengths, and vice versa. In contrast, for high gas fractions ($\varepsilon \geq 0.15$), the variation in wavelengths is smooth.

Several applications of these results for the studies of dynamical stability, structure and evolution of galaxies are discussed in Section 4. For example, we calculate the values of $Q_{s\text{-}g}$ versus radius for the Milky Way, and find that over most of the inner Galaxy the two-fluid galactic disc is close to

neutral or marginal equilibrium. We also show that a gas-rich galaxy (with $\varepsilon \geq 0.25$) can only be stable if it has a low surface density. This prediction agrees with the low surface density values observed for the typical gas-rich, late-type (Scd–Im) galaxies (e.g., Roberts & Haynes 1994), and also for the gas-rich, giant but low surface brightness galaxies such as Malin 1 (Impey & Bothun 1989).

Further, we predict that the gas-rich, late-type galaxies (and in fact all galaxies in the early stages of evolution) would show features covering a large range of wavelengths in *both* stars and gas. This may explain their patchy, fragmented appearance. A new regime explored here is that of low $\varepsilon \leq 0.1$, and low Q_g and high Q_s values, for which l_{s-g} is shown to be in the gas domain of small wavelengths – despite the small gas fractions. These parameters occur in the inner regions of early-type, gas-poor galaxies. Thus we can explain the multiple small arms seen in early-type galaxies such as NGC 2841 or 3898. Future high-resolution observations in the near-infrared and the mm-wave region would allow us to compare our results with sizes of features in stars and gas for a large number of external galaxies.

ACKNOWLEDGMENTS

It is a pleasure to thank the Astronomy Program, State University of New York at Stony Brook, USA for their hospitality during my sabbatical leave in 1993, when a part of this work was carried out.

REFERENCES

Bertin G., Romeo A., 1988, A&A, 195, 105
Binney J., Tremaine S., 1987, Galactic Dynamics. Princeton Univ. Press, Princeton
Bonazzola S., Falgarone E., Heyvaerts J., Perault M., Puget J. L., 1987, A&A, 172, 293
Bottema R. D., 1989, A&A, 221, 236
Burnside W. S., Panton A. W., 1960, Theory of Equations, Vol. 1. Dover, New York
Caldwell J. A. R., Ostriker J. P., 1981, ApJ, 251, 61
Chamcham K., Pitts E., Tayler R. J., 1993, MNRAS, 263, 967
Combes F., 1991, ARA&A, 29, 195
Elmegreen B. G., 1987, ApJ, 312, 626
Elmegreen B. G., 1992, in Bartholdi P., Pfenninger D., eds, The Galactic Interstellar Medium. Springer-Verlag, Berlin, p. 256
Evrard A. E., 1993, in Shull J. M., Thronson H. A., eds, The environment and evolution of galaxies. Kluwer, Dordrecht, p. 69
Fridman A. M., Polyachenko V. L., 1984, Physics of Gravitating Systems, Vol. I. Springer-Verlag, New York
Grishchuk L. P., Zel'dovich Ya. B., 1981, SvA, 25, 267
Goldreich P., Lynden-Bell D., 1965, MNRAS, 130, 125
Impey C., Bothun G., 1989, ApJ, 341, 89
Jog C. J., 1982, PhD thesis, State University of New York at Stony Brook, USA
Jog C. J., 1992, ApJ, 390, 378
Jog C. J., Ostriker J. P., 1988, ApJ, 328, 404
Jog C. J., Solomon P. M., 1984, ApJ, 276, 114 (JS1)
Jog C. J., Solomon P. M., 1984, ApJ, 276, 127 (JS2)
Kennicutt R. C., 1989, ApJ, 344, 685
Larson R. B., 1988, in Pudritz R. E., Fich M., eds, Galactic and Extragalactic Star Formation. Reidel, Dordrecht, p. 459
Lewis J. R., Freeman K. C., 1989, AJ, 97, 139
Lynden-Bell D., 1967, in Ehlers J., ed., Lectures in Applied Mathematics, Vol. 9. American Mathematical Society, Providence, p. 131
Nakamura T., 1978, Prog. Theoret. Phys., 59, 1129
Noguchi M., Shlosman I., 1993, ApJ, 390, 378
Roberts M. A., Haynes M. P., 1994, ARA&A, 32, 115
Safronov V. S., 1960, Ann d'Ap, 23, 979
Sandage A., 1961, The Hubble Atlas of Galaxies. Carnegie Institute of Washington, Washington
Sargent A. I., Welch J. E., 1993, ARA&A, 31, 297
Scoville N. Z., Sanders D. B., 1987, in Hollenbach D. J., Thronson H. A., eds, Interstellar Processes. Reidel, Dordrecht, p. 21
Sellwood J. A., Carlberg R. G., 1984, ApJ, 282, 61
Shlosman I., Begelman M. C., 1989, 341, 685
Smith B. F., Miller R. H., 1986, ApJ, 309, 535
Toomre A., 1964, ApJ, 139, 1217
Wang B., Silk J., 1994, ApJ, 427, 759
Young J. S., 1990, in Thronson H. A., Shull J. M., eds, The Interstellar Medium In Galaxies. Kluwer, Dordrecht, p. 67